Flexural effects in dynamic determination of pile capacity

Effets de flexion dans la détermination dynamique de la capacité portante d'un pieu

A. Holeyman[1], M. Allani
Université Catholique de Louvain, Louvain-la-Neuve. Belgique

ABSTRACT

The flexural vibration of piles during dynamic tests have to be investigated carefully. In this paper, we present two large scale case histories of high strain dynamic pile testing where eccentric impacts where generated. First, dynamic measured signals are presented to show the different quantities relationships (force, velocity, bending moment, and angular velocity). Then, flexural effects on the dynamic pile capacity are determined by wave reflexions.

RÉSUMÉ

L'analyse de la flexion des pieux lors de la mise en charge dynamique doit être minutieusement traitée. On présente dans cet article deux cas de chargement dynamique de pieu à grande déformation où un impact excentré à été généré. Nous analysons en premier lieu les signaux mesurés afin de mettre en valeur des différentes relations entre les paramètres (force, vitesse, moment fléchissant et vitesse angulaire). Les effets de flexion sur la capacité portante du pieu, évaluée sur base de réflexions d'ondes.

Keywords: Pile dynamics, flexural effects, Case Method

1 INTRODUCTION

Pile design analysis is needed to verify required functions (bearing capacity, allowable settlement, installation feasibility…). There are 3 types of dynamic pile tests: 1) high strain dynamic test, 2) high strain kinetic test, also known as "rapid load test" (with longer load application period comparing to classical high strain test) and 3) integrity test (short wavelength for better detection anomalies in the pile) [4]. We will focus in this paper on high strain dynamic testing where the main objective is to evaluate the dynamic and static bearing capacity of the pile. Static loading tests remain the reference for checking a pile performance since they best approach the real load in terms of duration and loading rate. Nevertheless, carrying out static tests takes a long time and involves a very expensive mobilization of the load and associated reaction. For these reasons dynamic loading tests (DLTs) have now been adopted by most engineering communities with the aim to improve productivity in term of quality control and design confirmation. These objectives seem to be satisfactorily achieved as the DLT test becomes more and more accepted as a routine procedure [3].

---

[1] Corresponding Author.

High strain dynamic pile testing consists in the measurement of pile strain and acceleration at the pile head under impacts of large weights. Pile strains and accelerations are measured with strain transducers and accelerometers, respectively.

However, it is worth noting that DLTs still include some limitations even though high technology and sophisticated interpretation are used during measurement and in signals post analysis. An important uncertainty or difficulty we may find in a DLT is the complex combination of compressive, tensile and also bending forces that may induce higher stresses than in service conditions and which may cause not only pile damage but also a signal mismatching that corresponding to a purely axial condition, as assumed for test interpretation.

Poskitt (1992), Holeyman (2000) and Charue (2004) indicate that eccentricity of the mass ram is often observed in DLTs. It is also well observed in pile driving where extreme conditions may be reached. Poskitt (1991, 1992 and 1996) was among the rare authors who addressed the problem of non axial effects in pile driving. To study the misalignment problem, he studied the general theory of impacts in two dimensions using Smith's 1960 model to represent the loading rate effects. However, no conclusions were derived concerning the flexural effects on the axial bearing capacity determination.

In this paper, case histories of pile dynamic testing under eccentric impacts are presented. First we present the Limelette and Tessenderlo sites geotechnical conditions and the experimental procedure. Then, axial and flexural signal analyses are performed with a focus on transferred energy to the pile and ram-pile misalignment effects. Finally, determination of static and dynamic pile capacity from dynamic measurements are developed. The Case method [4,9] is used for the calculation of shaft, base and total soil resistance. Conclusions about flexural effects on bearing capacity are finally made.

2 GEOTECHNICAL SITE DESCRIPTION AND EXPERIMENTAL PROCEDURE

In-situ dynamic pile tests were performed in Limelette and Tessenderlo sites, both located in Belgium. CPTs indicate that the stratigraphy consists of 8 m thickness of silt layer over Brussellian sand layer at Limelette while compact sandy silt prevails in the top 6 m over silt to clayey sand layer at Tessenderlo. Dynamic impacts on piles were generated using a Dynamic Loading Test Module. The system, called 'FondyTest', has been developed at the Department of Civil and Environmental Engineering of UCL. It consists in a 4 tonnes ram mass with an adjustable drop height, easily transportable to the field. The eccentricity of impact may also be controlled thanks to an automatic air cushion actuation. The actual eccentricity imposed to each blow might also be verified manually in the field.

A driven precast prestressed square concrete pile with $a = 35$ cm side and 9.5 m length was tested at the Limelette site. A continuous flight auger pile, with large hollow stem of diameter $2r = 60$ cm and about 15.5 m long was tested at the Tessenderlo site. Figure 1 presents the configuration of transducers for both sites with reference to pile axes, showing where four uniaxial piezoelectric accelerometers (Acc) and four strain gauges (Sg) were mounted.
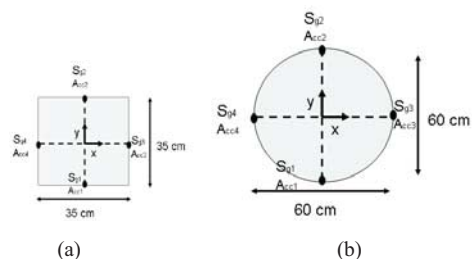
Figure 1: Sensors location at pile head for (a) Limelette and (b) Tessenderlo sites

From measured acceleration, one can obtain by integration the velocity and displacement at the pile head. Unfortunately, this is not an easy task as it seems because environmental signal noise, parasitic errors and offsetting integra-

tion problems affect the integration process. For noise elimination, a non-causal filtering (Butterworth type, 6th order with 1.5 kHz cutoff frequency) was used and a corrective constant velocity was incorporated in the signals to eliminate the integration offset. We have used PCB353B04 (500g) and PCB353M231 (5000g) accelerometer type to avoid traducers saturation based on maximum acceleration assessments. We also have considered high sampling frequencies at both sites to confirm Nyquist criteria; 20 kHz and 5 kHz for the Limelette and Tessenderlo sites respectively. For the calculation of applied force F, we used the formula: $F = EA_p \varepsilon_{mean}$ where E: is the pile Young modulus, A_p the pile cross section and $\varepsilon_{mean} = \sum_{i=1}^{n} \varepsilon_i / n$ is the mean strain measured within a cross-sectional plane.

Tables 1 and 2, summarize the sequential pile loading at both sites. H, e_x and e_y denote the drop heights and eccentricities. Eccentric impacts in x and y directions are generated at the Limelette site and only in y direction at the Tessenderlo site.

3   DYNAMIC SIGNAL ANALYSIS

3.1   Axial force, velocity and displacement relationships

In the very first moments of the impact, measured force and velocity times pile impedance I are superposed as functions of time (fig. 2). When the peak force F_{max} is correlated to the peak velocity V_{max} (fig. 3), the observed trend must reflect the nominal impedance of the pile I. The latter is equivalent to a dashpot factor modelling the behaviour of a semi-infinite pile subjected to an imposed velocity at its head: $I = \rho_{pile} c A_p$ where ρ_{pile} is the pile volumetric mass and $c = \sqrt{E / \rho_{pile}}$ is the bar wave propagation velocity. The 1.1 and 2.5 MN/m.s^{-1} values obtained by such regression confirm the impedance values expected from nominal properties of the impacted sections.

Table 1: Summary of impacts features, axial and flexural behavior, and dynamic soil resistance evaluations at the Limelette site.

Impact				Axial mode			Flexural mode			Dynamic resistance		
Blow n°	H (cm)	e_x (mm)	e_y (mm)	V_{max} (m/s)	F_{max} (kN)	E_{MAX} (kN.m)	M_{max}^y (kN.m)	$\dot{\theta}_{max}^y$ (rad/s)	E_{max}^y (kN.m)	R_f (MN)	Q_B (MN)	R_{dyn_case} (MN)
1,2	30	0	0	0.66	1.28	4.5	20.2	0.25	0.01	1.35	0.3	1.61
3	60	20	-20	1.65	2.19	15.5	53.1	0.62	0.07	1.80	0.9	2.68
4	40	20	-20	1.46	1.96	11.0	33.4	0.36	0.03	1.60	0.8	2.39
5	80	20	-20	2.06	2.67	23.1	42.0	0.42	0.05	1.84	1.2	3.01
6	80	20	-40	2.17	2.80	24.7	53.3	0.44	0.06	1.81	1.0	2.75
7,8	120	18	-32	2.66	3.36	36.6	113.0	1.10	0.16	1.85	1.1	2.85
9,10	80	22	-31	2.26	2.88	26.7	85.3	1.09	0.14	1.78	0.85	2.62
11	160	22	-31	3.16	4.04	52.3	123.2	1.90	0.15	1.91	1.13	3.04
12	40	2	-3	1.51	2.02	12.3	41.7	0.58	0.03	1.60	0.68	2.29
13	40	2	-40	1.55	1.99	12.3	42.6	0.51	0.02	1.59	0.7	2.30
14	40	3	-34	1.47	1.95	11.9	37.2	0.56	0.04	1.60	0.7	2.28
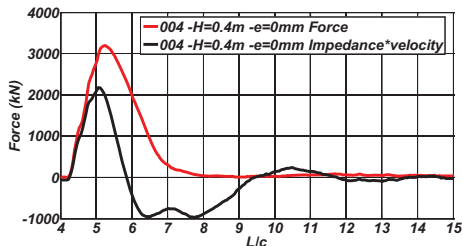
Figure 2: F and V*I signals at the Tessenderlo site
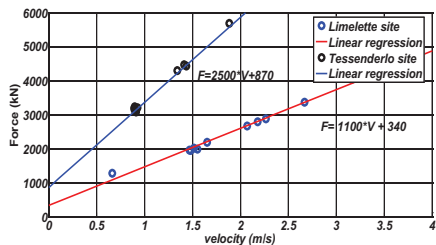
Figure 3: F_{max} and V_{max} Regression

Figure 4 presents the evolution of maximum and permanent settlements versus the hammer drop height at the Limelette site. The maximum settlement curve is characterized by a decreasing slope from the origin up to a given drop height beyond which a constant slope prevails. The permanent settlement curve is characterized by negligible values up to a given drop height called the 'critical height' beyond which maximum and permanent set-

tlement evolve as parallel curves, separated by a constant "rebound".
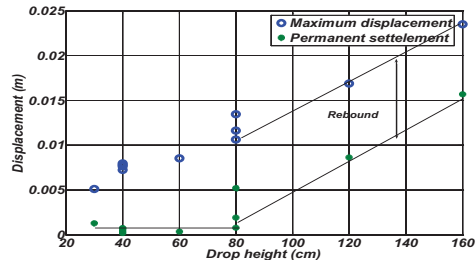
Figure 4: Permanent and maximum settlement versus drop height at the Limelette site.

3.2 Energy analysis

The axial energy transmitted to the pile (called 'Enthru') is defined as the integration over time of the product of force and velocity signals, until the end of impact t_f:

$$Enthru = \int_{0}^{t_f} F(t)V(t)dt$$

This term reflects the performance of the system which can be compared to the hammer potential energy (MgH). It can be concluded that the net energy transferred to the pile amounts to approximately 80% of the hammer potential energy.

Table 2: Impacts features, axial and flexural behavior, and dynamic soil resistance evaluations at the Tessenderlo site.

Impact			Axial mode			Flexural	Dynamic resistance		
Blow n°	H (cm)	e_y (mm)	V_{max} (m/s)	F_{max} (kN)	E_{MAX} (kN.m)	M_{max}^{y} (kN.m)	R_f (MN)	Q_B (MN)	R_{dyn_case} (MN)
1	70	0	1.34	4.29	17.0	38.3	3.09	3.24	6.22
2	110	0	1.88	5.69	3.0	38.2	3.70	4.60	8.14
3	40	0	0.89	3.19	9.8	37.7	2.42	2.14	4.62
4	40	37	0.89	3.13	9.7	-53.0	2.35	2.12	4.64
5	70	37	1.43	4.43	19.7	-61.7	3.02	3.44	6.61
6	40	62	0.91	3.08	9.9	-91.7	2.21	2.15	4.63
7	40	37	0.92	3.21	10.6	89.2	2.41	2.15	4.81
8	70	37	1.41	4.47	20.1	114.7	3.15	3.42	6.65
9	40	55	0.89	3.24	10.4	119.9	2.44	2.15	4.71

By analogy with the axial analysis we estimate the flexural energy transmitted to the pile using the relation:

$$Enthru_{flex} = \int_{0}^{t_f} M(t)\dot{\theta}(t)dt$$

where M is the bending moment at the pile head and $\dot{\theta}$ is the pile head cross section angular velocity.

The bending moment M^x (M^y) about the x- (y-) direction for both sites was calculated based on diametrically opposed measured strains (ε_1 and ε_2) on the pile head section. Bernoulli assumptions lead to $M = \dfrac{Ea^3}{12}(\varepsilon_2 - \varepsilon_1)$ and $M = \dfrac{E.\pi.r^3}{8}(\varepsilon_2 - \varepsilon_1)$ for a square and circular cross section, respectively.

Table 1 and 2 also contain axial and flexural data for the Limelette and Tessenderlo sites respectively. Large bending moments (more than 100 kN.m) are observed for both sites even though limited eccentricities are imposed. Furthermore, the dependency of the bending moment to the eccentricity is more pronounced than that to the drop height.

The 'Enthru$_{flex}$' signals are quite similar to the 'Enthru' energy signals. However, the ratio of the maximum flexural energy E^y_{max} to the maximum axial energy E_{MAX} is very small, typically of the order of 0.5% (Table 1).

4   DYNAMIC PILE CAPACITY DERTERMINATION

As already explained, pile impedance represents the proportionality between force and velocity for a free semi-infinite pile where no soil interaction is considered. For the pile base, the following expression can give some indication about the dynamic toe resistance if rigid plastic behavior is assumed [4]:

$$Q_B = \frac{1}{2}[F(t^+) + IV(t^+)] + \frac{1}{2}[F(t^+ + \frac{2L}{c})] - IV(t^+ + \frac{2L}{c})]$$

where t^+ is a time selected to obtain the maximum value of Q_B. The skin friction R_f mobilized down to the pile depth can be can be derived form the difference between force and velocity R_f =F-IV, reaching a maximum value at t^++2L/c.

The Case method (Goble et al 1975) is based on the difference between signals of a free pile and soil resistance perturbation:

$$R_{dyn\_case} = \frac{1}{2}[F(t^+) + F(t^+ + \frac{2L}{c})] + \frac{I}{2}[V(t^+) - V(t^+ + \frac{2L}{c})]$$

The total dynamic soil resistance is derived based on a rigid plastic soil model. For this reason, time t^+ is picked as to correspond to peak velocity V_{max}. Validity of this assumption especially for base modeling is discussed in Holeyman (1992) and Charue (2004). Total, base, and shaft soil resistance in Limelette and Tessenderlo sites are presented in Tables 1 and 2 respectively.

It was concluded that it seems reasonable to choose time t^+ at the time when first peak velocity occurs since soil resistance achieves a maximum value at that time. It was further confirmed that higher impacts mobilize more of the ultimately available soil resistance.

An increase can be noted in the total dynamic soil resistance under eccentric impacts, especially for the 70cm drop height at Tessenderlo (about 400kN increase) and for the 40 cm drop height at Limelette (about 200kN increase).

5   AXIAL AND FLEXURAL PILE RESPONSE

Several numerical models (TNOWAVE, CAPWAP, SIMBAT, NUSUM-UCL…) approach pile/soil interaction by a computer simulation with a view to reproduce measured force and velocity signals. Either the force or the velocity (or a combination of signals like the downward force wave) are imposed as a stimulus at the top boundary of the model (Charue 2004). The load-velocity trace (fig. 5) can be used to visually assess the quality of the optimizing procedure. The initial portion of the trace is linear and provides another evalua-

tion of the impedance of the piles (1.2 and 2.1 MN/ms^{-1}, respectively)

The same reasoning may also be applied to the flexural mode. Allani and Holeyman [2] elaborated a back calculation analysis to assess lateral soil stiffness and damping under steady state lateral pile loading. Lissajous type curves of experimental bending moment versus pile head angular velocity (fig. 6) allows one to graphically monitor the corresponding optimization procedure curve which is presently undergoing development.
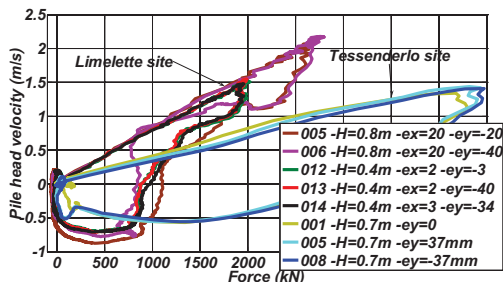
Figure 5: Axial load-velocity curves for Limelette and Tessenderlo sites.
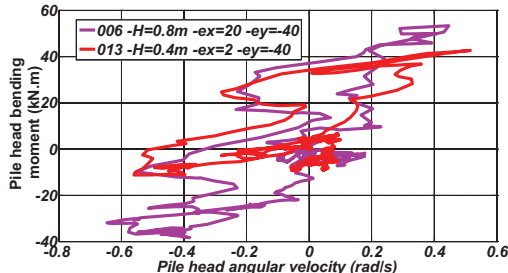
Figure 6: $M^y - \dot{\theta}^y$ curves at the Limelette site.

6   CONCLUSION

Two case histories of axial and flexural signal analysis in high strain dynamic pile tests have been presented. Although high eccentrici-

ty was applied during impacts, the transferred flexural energy remains very small compared to the axially transferred one. However, an increase of the Case determined dynamic soil resistance was observed under eccentric impacts at the Tessenderlo site. By analogy to the current axial analysis, a flexural response curve has been suggested at the pile head as a reference to deduce lateral soil stiffness and damping through a matching back-calculation algorithm.

REFERENCES

[1] M. Allani and A. Holeyman. Non axial effects in dynamic pile testing: Pile vibration analysis using Timoshenko beam theory. *Geotechnical Engineering 20, View of Young European Geotechnical Engineers*, Brno (2010), 158-163.

[2] M. Allani and A. Holeyman. Signal analysis of axial and flexural behavior in high strain dynamic pile testing. *Proceedings of the 2nd International conference on Geotechnical Engineering*, Hammamet, Tunisia (2010), 477-486.

[3] N. Charue, Loading rate effects on pile load-displacement behaviour derived from back calculation analysis of two load testing procedure, 2004.

[4] A. E. Holeyman, Keynote lecture: Technology of pile dynamics*, Application of Stress waves theory to piles* (2000), 195-215.

[5] T.J.Poskitt, Keynote lecture: problems of reconciling stress wave measurements with theory *application of Stress Waves theory to piles, Rotterdam,* 1992.

[6] T.J.Poskitt, Energy losses in pile-driving due to soil rate effects and hammer misalignment, P*roc Instn Engrs* **2**, 1991, 823-851.

[7] F. Rausche, G.G. Goble, G.E. Likins, Dynamic determination of pile capacity, *Journal of geotechnical Engineering*, **11** (1985), 367-383.

[8] G. VanAlboom, and V. Whenham, Soil investigation campaign at Limelette (Belgium) Results. In Proceeding of the Symposium on screw piles in sand. Design and recent development (2003), Swts and Zeitlinger, Eds.

[9] S. Yao and T. Nogami, Lateral cyclic response on pile in viscoelastic Winkler subgrade. Journal of engeneering mechanics **120** (1994), 758-775.